

Higher-Order Low-Rank Regression

Guillaume Rabusseau* Hachem Kadri
Aix-Marseille University

February 23, 2016

Abstract

This paper proposes an efficient algorithm (HOLRR) to handle regression tasks where the outputs have a tensor structure. We formulate the regression problem as the minimization of a least square criterion under a multilinear rank constraint, a difficult non convex problem. HOLRR computes efficiently an approximate solution of this problem, with solid theoretical guarantees. A kernel extension is also presented. Experiments on synthetic and real data show that HOLRR outperforms multivariate and multilinear regression methods and is considerably faster than existing tensor methods.

1 Introduction

Recently, there has been an increasing interest in adapting machine learning and statistical methods to tensors. Data with a natural tensor structure is encountered in many scientific areas including neuroimaging (Zhou et al., 2013), signal processing (Cichocki et al., 2009), spatio-temporal analysis (Bahadori et al., 2014) and computer vision (Lu et al., 2013). Extending multivariate regression methods to tensors is one of the challenging task in this area. Most existing works extend linear models to the multilinear setting and focus on the tensor structure of the input data (e.g. Signoretto et al. (2013)). Little has been done however to investigate learning methods for *tensor-structured output data*.

We consider a multilinear regression task where inputs are vectors and outputs are tensors. In order to leverage the tensor structure of the output data, we formulate the problem as the minimization of a least squares criterion subject to a *multilinear rank* constraint on the regression tensor. The rank constraint enforces the model to capture the low-rank structure of the outputs and to explain the dependencies between inputs and outputs in a low-dimensional multilinear subspace.

Unlike previous work we do not use a convex relaxation of this difficult non-convex optimization problem. Instead we design an efficient approximation algorithm (HOLRR) for which we are able to provide good approximation

*Contact author: guillaume.rabusseau@lif.univ-mrs.fr.

guarantees. We also present a kernelized version of HOLRR which extends our model to the nonlinear setting. Experiments on synthetic and real data shows that HOLRR obtains better predictive accuracy while being computationally very competitive. We also present an image recovery experiment which gives an illustrative insight on the effects of multilinear rank regularization.

Related work. In the context of multi-task learning, [Romera-Paredes et al. \(2013\)](#) have proposed a linear model using a tensor-rank penalization of a least squares criterion to take into account the multi-modal interactions between tasks. Their approach relies on a convex relaxation of the multilinear rank constraint using the trace norms of the matricizations. They also propose a non-convex approach (MLMT-NC) but it is computationally very expensive. [Bahadori et al. \(2014\)](#) have proposed a greedy algorithm to solve a low-rank tensor learning problem in the context of multivariate spatio-temporal data analysis. The linear model they assume is different from the one we propose, it is specifically designed for spatio-temporal data and does not fit into the general tensor-valued regression framework we consider here.

Paper outline. We provide some background on low-rank regression and tensors in Section 2. In Section 3 we introduce the tensor response regression problem, we develop the HOLRR algorithm to tackle the minimization problem with multilinear rank constraint, and we prove that this algorithm has good approximation guarantees. A kernelized version of HOLRR is provided in Section 4. Finally, we assess the performances of our method through simulation study and real data analysis in Section 5.

2 Preliminaries

We begin by introducing some notations. For any integer k we use $[k]$ to denote the set of integers from 1 to k . We use lower case bold letters for vectors (e.g. $\mathbf{v} \in \mathbb{R}^{d_1}$), upper case bold letters for matrices (e.g. $\mathbf{M} \in \mathbb{R}^{d_1 \times d_2}$) and bold calligraphic letters for higher order tensors (e.g. $\mathcal{T} \in \mathbb{R}^{d_1 \times d_2 \times d_3}$). The identity matrix will be written as \mathbf{I} . The i th row (resp. column) of a matrix \mathbf{M} will be denoted by $\mathbf{M}_{i,:}$ (resp. $\mathbf{M}_{:,i}$). This notation is extended to slices of a tensor in the straightforward way. If $\mathbf{v} \in \mathbb{R}^{d_1}$ and $\mathbf{v}' \in \mathbb{R}^{d_2}$, we use $\mathbf{v} \otimes \mathbf{v}' \in \mathbb{R}^{d_1 \cdot d_2}$ to denote the Kronecker product between vectors, and its straightforward extension to matrices and tensors. Given a matrix $\mathbf{M} \in \mathbb{R}^{d_1 \times d_2}$, we use $\text{vec}(\mathbf{M}) \in \mathbb{R}^{d_1 \cdot d_2}$ to denote the column vector obtained by concatenating the columns of \mathbf{M} .

2.1 Tensors and Tucker Decomposition

We first recall some basic definitions of tensor algebra; more details can be found in [Kolda & Bader \(2009\)](#). A *tensor* $\mathcal{T} \in \mathbb{R}^{d_1 \times \dots \times d_p}$ is a collection of real numbers ($\mathcal{T}_{i_1, \dots, i_p} : i_n \in [d_n], n \in [p]$). The *mode- n* fibers of \mathcal{T} are the vectors obtained by fixing all indices except for the n th one, e.g. $\mathcal{T}_{:,i_2, \dots, i_p} \in \mathbb{R}^{d_1}$.

The n th *mode matricization* of \mathcal{T} is the matrix having the mode- n fibers of \mathcal{T} for columns and is denoted by $\mathbf{T}_{(n)} \in \mathbb{R}^{d_n \times d_1 \cdots d_{n-1} d_{n+1} \cdots d_p}$. The vectorization of a tensor is defined by $\text{vec}(\mathcal{T}) = \text{vec}(\mathbf{T}_{(1)})$. The *inner product* between two tensors \mathcal{S} and \mathcal{T} (of the same size) is defined by $\langle \mathcal{S}, \mathcal{T} \rangle = \langle \text{vec}(\mathcal{S}), \text{vec}(\mathcal{T}) \rangle$ and the Frobenius norm is defined by $\|\mathcal{T}\|_F^2 = \langle \mathcal{T}, \mathcal{T} \rangle$. In the following \mathcal{T} always denotes a tensor of size $d_1 \times \cdots \times d_p$.

mode- n product. The *mode- n matrix product* of the tensor \mathcal{T} and a matrix $\mathbf{X} \in \mathbb{R}^{m \times d_n}$ is a tensor denoted by $\mathcal{T} \times_n \mathbf{X}$. It is of size $d_1 \times \cdots \times d_{n-1} \times m \times d_{n+1} \times \cdots \times d_p$ and is defined by the relation $\mathcal{Y} = \mathcal{T} \times_n \mathbf{X} \Leftrightarrow \mathbf{Y}_{(n)} = \mathbf{X} \mathbf{T}_{(n)}$. The *mode- n vector product* of the tensor \mathcal{T} and a vector $\mathbf{v} \in \mathbb{R}^{d_n}$ is a tensor defined by $\mathcal{T} \bullet_n \mathbf{v} = \mathcal{T} \times_n \mathbf{v}^\top \in \mathbb{R}^{d_1 \times \cdots \times d_{n-1} \times d_{n+1} \times \cdots \times d_p}$. Given tensors \mathcal{S} and \mathcal{T} and matrices \mathbf{X}, \mathbf{A} and \mathbf{B} , it is easy to check that $\langle \mathcal{T} \times_n \mathbf{X}, \mathcal{S} \rangle = \langle \mathcal{T}, \mathcal{S} \times_n \mathbf{X}^\top \rangle$ and $(\mathcal{T} \times_n \mathbf{A}) \times_n \mathbf{B} = \mathcal{T} \times_n \mathbf{B} \mathbf{A}$ (where we assumed conforming dimensions of the tensors and matrices).

Multilinear rank. The *mode- n rank* of \mathcal{T} is the dimension of the space spanned by its mode- n fibers, that is $\text{rank}_n(\mathcal{T}) = \text{rank}(\mathbf{T}_{(n)})$. The *multilinear rank* of \mathcal{T} , denoted by $\text{rank}(\mathcal{T})$, is the tuple of mode- n ranks of \mathcal{T} : $\text{rank}(\mathcal{T}) = (R_1, \cdots, R_p)$ where $R_n = \text{rank}_n(\mathcal{T})$ for $n \in [p]$. We will write $\text{rank}(\mathcal{T}) \leq (S_1, \cdots, S_p)$ whenever $\text{rank}_1(\mathcal{T}) \leq S_1, \text{rank}_2(\mathcal{T}) \leq S_2, \cdots, \text{rank}_p(\mathcal{T}) \leq S_p$.

Tucker decomposition. The *Tucker decomposition* is a form of higher-order principal component analysis. It decomposes a tensor \mathcal{T} into a core tensor \mathcal{G} transformed by an orthogonal matrix along each mode:

$$\mathcal{T} = \mathcal{G} \times_1 \mathbf{U}_1 \times_2 \mathbf{U}_2 \times_3 \cdots \times_p \mathbf{U}_p, \quad (1)$$

where $\mathcal{G} \in \mathbb{R}^{R_1 \times R_2 \times \cdots \times R_p}$, $\mathbf{U}_i \in \mathbb{R}^{d_i \times R_i}$ for $i \in [p]$ and $\mathbf{U}_i^\top \mathbf{U}_i = \mathbf{I}$ for all $i \in [p]$. The number of parameters involved in a Tucker decomposition can be considerably smaller than $d_1 d_2 \cdots d_p$. We have the following identities when matricizing and vectorizing a Tucker decomposition

$$\begin{aligned} \mathbf{T}_{(n)} &= \mathbf{U}_n \mathbf{G}_{(n)} (\mathbf{U}_p \otimes \cdots \otimes \mathbf{U}_{n+1} \otimes \mathbf{U}_{n-1} \otimes \cdots \otimes \mathbf{U}_1)^\top \\ \text{vec}(\mathcal{T}) &= (\mathbf{U}_p \otimes \mathbf{U}_{p-1} \otimes \cdots \otimes \mathbf{U}_1) \text{vec}(\mathcal{G}). \end{aligned} \quad (2)$$

It is well known that \mathcal{T} admits the Tucker decomposition (1) if and only if $\text{rank}(\mathcal{T}) \leq (R_1, \cdots, R_p)$ (see e.g. Kolda & Bader (2009)). Finding an exact Tucker decomposition can be done using the higher-order SVD algorithm (HOSVD) introduced by De Lathauwer et al. (2000). Although finding the best approximation of multilinear rank (R_1, \cdots, R_p) of a tensor \mathcal{T} is a difficult problem, the truncated HOSVD algorithm provides good approximation guarantees and often performs well in practice.

2.2 Low-Rank Regression

Multivariate regression is the task of recovering a function $f : \mathbb{R}^d \rightarrow \mathbb{R}^p$ from a set of input-output pairs $\{(\mathbf{x}^{(n)}, \mathbf{y}^{(n)})\}_{n=1}^N$, where the outputs are sampled from the model with an additive noise $\mathbf{y} = f(\mathbf{x}) + \boldsymbol{\varepsilon}$, where $\boldsymbol{\varepsilon}$ is the error term. To solve this problem, the *ordinary least squares* (OLS) approach assumes a linear dependence between input and output data and boils down to finding a matrix $\mathbf{W} \in \mathbb{R}^{d \times p}$ that minimizes the squared error $\|\mathbf{X}\mathbf{W} - \mathbf{Y}\|_F^2$, where $\mathbf{X} \in \mathbb{R}^{N \times d}$ and $\mathbf{Y} \in \mathbb{R}^{N \times p}$ denote the input and the output matrices. To prevent overfitting and to avoid numerical instabilities a ridge regularization term (i.e. $\gamma\|\mathbf{W}\|_F^2$) is often added to the objective function, leading to the *regularized least squares* (RLS) method. The main drawback of this method is that it does not take into account the dependencies between the components of the response. It performs poorly when the outputs are correlated and the true dimension of the response is less than p . Indeed, it is easy to see that the OLS/RLS approach in the multivariate setting is equivalent to performing p linear regressions for each scalar output $\{\mathbf{y}_j\}_{j=1}^p$ independently.

Low-rank regression (or reduced-rank regression) addresses this issue by solving the following rank penalized problem

$$\min_{\mathbf{W} \in \mathbb{R}^{d \times p}} \|\mathbf{X}\mathbf{W} - \mathbf{Y}\|_F^2 + \gamma\|\mathbf{W}\|_F^2 \text{ s.t. } \text{rank}(\mathbf{W}) \leq R, \quad (3)$$

for a given integer R .

Suppose that $f(\mathbf{x}) = \mathbf{W}\mathbf{x}$. The constraint $\text{rank}(\mathbf{W}) = R$ implies linear restrictions on \mathbf{W} , i.e. there must exist $p - R$ linearly independent vectors $\mathbf{v}_1, \dots, \mathbf{v}_{p-R} \in \mathbb{R}^p$ such that $\mathbf{W}\mathbf{v}_i = \mathbf{0}$, which, in turn, implies that $\mathbf{y}^\top \mathbf{v}_i = \boldsymbol{\varepsilon}^\top \mathbf{v}_i$ for each $i \in [p - R]$. Intuitively this means that the linear subspace generated by the \mathbf{v}_i 's only contains noise. Another way to see this is to write $\mathbf{W} = \mathbf{A}\mathbf{B}$ with $\mathbf{A} \in \mathbb{R}^{d \times R}$ and $\mathbf{B} \in \mathbb{R}^{R \times p}$, which implies that the relation between \mathbf{x} and \mathbf{y} is explained in an R -dimensional latent space.

The rank constraint in (3) was first proposed in (Anderson, 1951), whereas the term *reduced-rank regression* was introduced in (Izenman, 1975). Adding a ridge regularization to the rank penalized problem was proposed in Mukherjee & Zhu (2011). In the rest of the paper we will refer to this approach as low-rank regression (LRR). The solution of minimization problem (3) is given by projecting the RLS solution onto the space spanned by the top R eigenvectors of $\mathbf{Y}^\top \mathbf{P} \mathbf{Y}$ where \mathbf{P} is the orthogonal projection matrix onto the column space of \mathbf{X} , that is $\mathbf{W}_{LRR} = \mathbf{W}_{RLS} \mathbf{\Pi}$ where $\mathbf{\Pi}$ is the matrix of the aforementioned projection. For more description and discussion of reduced-rank regression, we refer the reader to the books of Reinsel & Velu (1998) and Izenman (2008).

3 Low-Rank Regression for Tensor-Valued Functions

3.1 Problem Formulation

We consider a multivariate regression task where the response has a tensor structure. Let $f : \mathbb{R}^{d_0} \rightarrow \mathbb{R}^{d_1 \times d_2 \times \dots \times d_p}$ be the function we want to learn from a sample of input-output data $\{(\mathbf{x}^{(n)}, \mathcal{Y}^{(n)})\}_{n=1}^N$ drawn from the model $\mathcal{Y} = f(\mathbf{x}) + \mathcal{E}$, where \mathcal{E} is an error term. We assume that the function f is linear, that is $f(\mathbf{x}) = \mathcal{W} \bullet_1 \mathbf{x}$ for some regression tensor $\mathcal{W} \in \mathbb{R}^{d_0 \times d_1 \times \dots \times d_p}$. Note that the vectorization of this relation leads to $\text{vec}(f(\mathbf{x})) = \mathbf{W}_{(1)}^\top \mathbf{x}$ showing that this model is equivalent to the standard multivariate linear model.

Vectorization of the outputs. One way to tackle this linear regression task for tensor responses would be to vectorize each output sample and to perform a standard multivariate low-rank regression on the data $\{(\mathbf{x}^{(n)}, \text{vec}(\mathcal{Y}^{(n)}))\}_{n=1}^N \subset \mathbb{R}^{d_0} \times \mathbb{R}^{d_1 \dots d_p}$. A major drawback of this approach is that the tensor structure of the output is lost in the vectorization step. The low-rank model tries to capture linear dependencies between components of the output but it ignores *higher level dependencies* that could be present in a tensor-structured output. For illustration, suppose the output is a matrix encoding the samples of d_1 continuous variables at d_2 different time steps, one could expect structural relations between the d_1 time series, for example linear dependencies between the rows of the output matrix.

Low-rank regression for tensor responses. To overcome the limitation described above we propose an extension of the low-rank regression method for tensor-structured responses by enforcing low multilinear rank of the regression tensor \mathcal{W} . Let $\{(\mathbf{x}^{(n)}, \mathcal{Y}^{(n)})\}_{n=1}^N \subset \mathbb{R}^{d_0} \times \mathbb{R}^{d_1 \times d_2 \times \dots \times d_p}$ be a training sample of input/output data drawn from the model $f(\mathbf{x}) = \mathcal{W} \bullet_1 \mathbf{x} + \mathcal{E}$ where \mathcal{W} is assumed of low multilinear rank. Considering the framework of empirical risk minimization, we want to find a low-rank regression tensor \mathcal{W} minimizing the loss on the training data. To avoid numerical instabilities and to prevent overfitting we add a ridge regularization to the objective function, leading to the following minimization problem

$$\begin{aligned} \min_{\mathcal{W} \in \mathbb{R}^{d_0 \times \dots \times d_p}} \sum_{n=1}^N \ell(\mathcal{W} \bullet_1 \mathbf{x}^{(n)}, \mathcal{Y}^{(n)}) + \gamma \|\mathcal{W}\|_F^2 \quad (4) \\ \text{s.t. } \text{rank}(\mathcal{W}) \leq (R_0, R_1, \dots, R_p) , \end{aligned}$$

for some given integers R_0, R_1, \dots, R_p and where ℓ is a loss function. In this paper, we consider the squared error loss between tensors defined by $\ell(\mathcal{T}, \hat{\mathcal{T}}) =$

$\|\mathcal{T} - \hat{\mathcal{T}}\|_F^2$. Using this loss we can rewrite problem (4) as

$$\begin{aligned} \min_{\mathcal{W} \in \mathbb{R}^{d_0 \times d_1 \times \dots \times d_p}} \|\mathcal{W} \times_1 \mathbf{X} - \mathcal{Y}\|_F^2 + \gamma \|\mathcal{W}\|_F^2 \\ \text{s.t. } \text{rank}(\mathcal{W}) \leq (R_0, R_1, \dots, R_p) , \end{aligned} \quad (5)$$

where the input matrix $\mathbf{X} \in \mathbb{R}^{N \times d_0}$ and the output tensor $\mathcal{Y} \in \mathbb{R}^{N \times d_1 \times \dots \times d_p}$ are defined by $\mathbf{X}_{n,:} = (\mathbf{x}^{(n)})^\top$, $\mathcal{Y}_{n,:,\dots,:} = \mathcal{Y}^{(n)}$ for $n = 1, \dots, N$ (\mathcal{Y} is the tensor obtained by stacking the output tensors along the first mode).

Low-rank regression function. Let \mathcal{W}^* be a solution of problem (5), it follows from the multilinear rank constraint that $\mathcal{W}^* = \mathcal{G} \times_1 \mathbf{U}_0 \times_2 \dots \times_{p+1} \mathbf{U}_p$ for some core tensor $\mathcal{G} \in \mathbb{R}^{R_0 \times \dots \times R_p}$ and orthogonal matrices $\mathbf{U}_i \in \mathbb{R}^{d_i \times R_i}$ for $0 \leq i \leq p$. The regression function $f^* : \mathbf{x} \mapsto \mathcal{W}^* \bullet_1 \mathbf{x}$ can thus be written as

$$f^* : \mathbf{x} \mapsto \mathcal{G} \times_1 \mathbf{x}^\top \mathbf{U}_0 \times_2 \dots \times_{p+1} \mathbf{U}_p .$$

This implies several interesting properties. First, for any $\mathbf{x} \in \mathbb{R}^{d_0}$ we have $f^*(\mathbf{x}) = \mathcal{T}_{\mathbf{x}} \times_1 \mathbf{U}_1 \times_2 \dots \times_p \mathbf{U}_p$ with $\mathcal{T}_{\mathbf{x}} = \mathcal{G} \bullet_1 \mathbf{U}_0^\top \mathbf{x}$, which implies $\text{rank}(f^*(\mathbf{x})) \leq (R_1, \dots, R_p)$, that is the image of f^* is a set of tensors with low multilinear rank. Second, the relation between \mathbf{x} and $\mathcal{Y} = f^*(\mathbf{x})$ is explained in a low dimensional subspace of size $R_0 \times R_1 \times \dots \times R_p$. Indeed one can decompose the mapping f^* into the following steps: (i) project \mathbf{x} in \mathbb{R}^{R_0} as $\bar{\mathbf{x}} = \mathbf{U}_0^\top \mathbf{x}$, (ii) perform a low-dimensional mapping $\bar{\mathcal{Y}} = \mathcal{G} \bullet_1 \bar{\mathbf{x}}$, (iii) project back into the output space to get $\mathcal{Y} = \bar{\mathcal{Y}} \times_1 \mathbf{U}_1 \times_2 \dots \times_p \mathbf{U}_p$.

Comparison with LRR. First, it is obvious that the function learned by vectorizing the outputs and performing LRR does not enforce any multilinear structure in the predictions. That is, the tensor obtained by reshaping a vectorized prediction will not necessarily have a low multilinear rank. This is well illustrated in the experiment from Section 5.2 where this fact is particularly striking when we try to learn an image from noisy measurements with a rank constraint set to 1 (see Figure 2, left). Second, since the multilinear rank is defined with respect to the ranks of the matricizations there are some scenarios where the rank constraint in LRR after vectorizing the output will be (almost) equivalent to the multilinear rank constraint in (5). This is clear if the regression tensor is of low mode-1 rank and of full mode- n rank for $n > 1$, but even when $R_0 \ll R_i$ for $i \geq 1$ we can expect LRR to be able to capture most of the low-rank structure which is concentrated along the first mode.

3.2 Higher-Order Low-Rank Regression

We now propose an efficient algorithm to tackle problem (5). Theoretical approximation guarantees are given in the next section.

Problem reformulation. We first show that the ridge regularization term in (5) can be incorporated in the data fitting term. Let $\tilde{\mathbf{X}} \in \mathbb{R}^{(N+d_0) \times d_0}$ and $\tilde{\mathbf{Y}} \in \mathbb{R}^{(N+d_0) \times d_1 \times \dots \times d_p}$ be defined by $\tilde{\mathbf{X}}^\top = (\mathbf{X} \mid \gamma \mathbf{I})^\top$ and $\tilde{\mathbf{Y}}_{(1)}^\top = (\mathbf{Y}_{(1)} \mid \mathbf{0})^\top$. It is easy to check that the objective function in (5) is equal to $\|\mathcal{W} \times_1 \tilde{\mathbf{X}} - \tilde{\mathbf{Y}}\|_F^2$. Minimization problem (5) can then be rewritten as

$$\begin{aligned} \min_{\substack{\mathcal{G} \in \mathbb{R}^{R_0 \times R_1 \times \dots \times R_p}, \\ \mathbf{U}_i \in \mathbb{R}^{d_i \times R_i} \text{ for } 0 \leq i \leq p}} \|\mathcal{W} \times_1 \tilde{\mathbf{X}} - \tilde{\mathbf{Y}}\|_F^2 & \quad (6) \\ \text{s.t. } \mathcal{W} = \mathcal{G} \times_1 \mathbf{U}_0 \times_2 \mathbf{U}_1 \cdots \times_{p+1} \mathbf{U}_p, \\ \mathbf{U}_i^\top \mathbf{U}_i = \mathbf{I} \text{ for } 0 \leq i \leq p . \end{aligned}$$

We now show that this minimization problem can be reduced to finding $p+1$ projection matrices onto subspaces of dimension R_0, R_1, \dots, R_p . We start by showing that the core tensor \mathcal{G} solution of (6) is determined by the factor matrices $\mathbf{U}_0, \dots, \mathbf{U}_p$.

Theorem 1. For given orthogonal matrices $\mathbf{U}_0, \dots, \mathbf{U}_p$ the tensor \mathcal{G} that minimizes (6) is given by

$$\mathcal{G} = \tilde{\mathbf{Y}} \times_1 (\mathbf{U}_0^\top \tilde{\mathbf{X}}^\top \tilde{\mathbf{X}} \mathbf{U}_0)^{-1} \mathbf{U}_0^\top \tilde{\mathbf{X}}^\top \times_2 \mathbf{U}_1^\top \times_3 \cdots \times_{p+1} \mathbf{U}_p^\top .$$

Proof. Using Eq. 2 the objective function in (6) can be written as

$$\|(\mathbf{U}_p \otimes \mathbf{U}_{p-1} \otimes \cdots \otimes \mathbf{U}_1 \otimes \tilde{\mathbf{X}} \mathbf{U}_0) \text{vec}(\mathcal{G}) - \text{vec}(\tilde{\mathbf{Y}})\|_F^2 .$$

Let $\mathbf{M} = \mathbf{U}_p \otimes \mathbf{U}_{p-1} \otimes \cdots \otimes \mathbf{U}_1 \otimes \tilde{\mathbf{X}} \mathbf{U}_0$. The solution w.r.t. $\text{vec}(\mathcal{G})$ of this classical linear least-squares problem is given by $(\mathbf{M}^\top \mathbf{M})^{-1} \mathbf{M}^\top$. Using the mixed-product and inverse properties of the Kronecker product and the column-wise orthogonality of $\mathbf{U}_1, \dots, \mathbf{U}_p$ we obtain

$$\text{vec}(\mathcal{G}) = (\mathbf{U}_p \otimes \cdots \otimes \mathbf{U}_1 \otimes (\mathbf{U}_0^\top \tilde{\mathbf{X}}^\top \tilde{\mathbf{X}} \mathbf{U}_0)^{-1} \mathbf{U}_0^\top \tilde{\mathbf{X}}^\top) \text{vec}(\tilde{\mathbf{Y}}) . \quad \square$$

It follows from Theorem 1 that problem (5) can be written as

$$\begin{aligned} \min_{\substack{\mathbf{U}_i \in \mathbb{R}^{d_i \times R_i}, \\ 0 \leq i \leq p}} \|\tilde{\mathbf{Y}} \times_1 \mathbf{\Pi}_0 \times_2 \cdots \times_{p+1} \mathbf{\Pi}_p - \tilde{\mathbf{Y}}\|_F^2 & \quad (7) \\ \text{s.t. } \mathbf{U}_i^\top \mathbf{U}_i = \mathbf{I} \text{ for } 0 \leq i \leq p, \\ \mathbf{\Pi}_0 = \tilde{\mathbf{X}} \mathbf{U}_0 (\mathbf{U}_0 \tilde{\mathbf{X}}^\top \tilde{\mathbf{X}} \mathbf{U}_0^\top)^{-1} \mathbf{U}_0^\top \tilde{\mathbf{X}}^\top, \\ \mathbf{\Pi}_i = \mathbf{U}_i \mathbf{U}_i^\top \text{ for } 1 \leq i \leq p , \end{aligned}$$

where we used $\mathcal{W} \times_1 \tilde{\mathbf{X}} = \tilde{\mathbf{Y}} \times_1 \mathbf{\Pi}_0 \times_2 \cdots \times_{p+1} \mathbf{\Pi}_p$. Note that $\mathbf{\Pi}_0$ is the orthogonal projection onto the space spanned by the columns of $\tilde{\mathbf{X}} \mathbf{U}_0$ and $\mathbf{\Pi}_i$ is the orthogonal projection onto the column space of \mathbf{U}_i for $i \geq 1$. Hence solving problem (5) is equivalent to finding $p+1$ low-dimensional subspaces U_0, \dots, U_p such that projecting $\tilde{\mathbf{Y}}$ onto the spaces $\tilde{\mathbf{X}} U_0, U_1, \dots, U_p$ along the corresponding modes is close to $\tilde{\mathbf{Y}}$.

HOLRR algorithm. Since solving problem (7) for the $p+1$ projections simultaneously is a difficult non-convex optimization problem we propose to solve it independently for each projection. This approach has the benefits of both being computationally efficient and providing good theoretical approximation guarantees (see Theorem 2). The following proposition gives the analytic solutions of (7) when each projection is considered independently.

Proposition 1. For $0 \leq i \leq p$, using the definition of $\mathbf{\Pi}_i$ in (7), the optimal solution of

$$\min_{\mathbf{U}_i \in \mathbb{R}^{d_i \times R_i}} \|\tilde{\mathcal{Y}} \times_{i+1} \mathbf{\Pi}_i - \tilde{\mathcal{Y}}\|_F^2 \text{ s.t. } \mathbf{U}_i^\top \mathbf{U}_i = \mathbf{I}$$

is given by the eigenvectors of

$$\begin{cases} (\tilde{\mathbf{X}}^\top \tilde{\mathbf{X}})^{-1} \tilde{\mathbf{X}}^\top \tilde{\mathbf{Y}}_{(1)} \tilde{\mathbf{Y}}_{(1)}^\top \tilde{\mathbf{X}} & \text{if } i = 0 \\ \tilde{\mathbf{Y}}_{(i)} \tilde{\mathbf{Y}}_{(i)}^\top & \text{otherwise} \end{cases}$$

that corresponds to the R_i largest eigenvalues.

Proof. For any $0 \leq i \leq p$, since $\mathbf{\Pi}_i$ is a projection we have $\langle \tilde{\mathcal{Y}} \times_1 \mathbf{\Pi}_i, \tilde{\mathcal{Y}} \rangle = \langle \mathbf{\Pi}_i \tilde{\mathbf{Y}}_{(i)}, \tilde{\mathbf{Y}}_{(i)} \rangle = \|\mathbf{\Pi}_i \tilde{\mathbf{Y}}_{(i)}\|_F^2$, thus minimizing $\|\tilde{\mathcal{Y}} \times_i \mathbf{\Pi}_i - \tilde{\mathcal{Y}}\|_F^2$ is equivalent to minimizing $\|\mathbf{\Pi}_i \tilde{\mathbf{Y}}_{(i)}\|_F^2 - 2\langle \mathbf{\Pi}_i \tilde{\mathbf{Y}}_{(i)}, \tilde{\mathbf{Y}}_{(i)} \rangle = -\|\mathbf{\Pi}_i \tilde{\mathbf{Y}}_{(i)}\|_F^2$. For $i \geq 1$, we have $\|\mathbf{\Pi}_i \tilde{\mathbf{Y}}_{(i)}\|_F^2 = \text{Tr}(\mathbf{U}_i^\top \tilde{\mathbf{Y}}_{(i)} \tilde{\mathbf{Y}}_{(i)}^\top \mathbf{U}_i)$ which is maximized by letting the columns of \mathbf{U}_i be the top R_i eigenvectors of the matrix $\tilde{\mathbf{Y}}_{(i)} \tilde{\mathbf{Y}}_{(i)}^\top$. For $i = 0$ we have

$$\|\mathbf{\Pi}_0 \tilde{\mathbf{Y}}_{(1)}\|_F^2 = \text{Tr}(\mathbf{\Pi}_0 \tilde{\mathbf{Y}}_{(1)} \tilde{\mathbf{Y}}_{(1)}^\top \mathbf{\Pi}_0^\top) = \text{Tr}((\mathbf{U}_0^\top \mathbf{A} \mathbf{U}_0)^{-1} \mathbf{U}_0^\top \mathbf{B} \mathbf{U}_0)$$

with $\mathbf{A} = \tilde{\mathbf{X}}^\top \tilde{\mathbf{X}}$ and $\mathbf{B} = \tilde{\mathbf{X}}^\top \tilde{\mathbf{Y}}_{(1)} \tilde{\mathbf{Y}}_{(1)}^\top \tilde{\mathbf{X}}$, which is maximized by the top R_0 eigenvectors of $\mathbf{A}^{-1} \mathbf{B}$. \square

The results from Theorem 1 and Proposition 1 can be rewritten using the original input matrix \mathbf{X} and output tensor \mathcal{Y} . Since $\tilde{\mathbf{X}}^\top \tilde{\mathbf{X}} = \mathbf{X}^\top \mathbf{X} + \gamma \mathbf{I}$ and $\tilde{\mathcal{Y}} \times_1 \tilde{\mathbf{X}}^\top = \mathcal{Y} \times_1 \mathbf{X}^\top$, we can rewrite the solution of Theorem 1 as

$$\mathcal{G} = \mathcal{Y} \times_1 (\mathbf{U}_0^\top (\mathbf{X}^\top \mathbf{X} + \gamma \mathbf{I}) \mathbf{U}_0)^{-1} \mathbf{U}_0^\top \mathbf{X}^\top \times_2 \mathbf{U}_1^\top \times_3 \cdots \times_{p+1} \mathbf{U}_p^\top .$$

Similarly for Proposition 1 we have

$$(\tilde{\mathbf{X}}^\top \tilde{\mathbf{X}})^{-1} \tilde{\mathbf{X}}^\top \tilde{\mathbf{Y}}_{(1)} \tilde{\mathbf{Y}}_{(1)}^\top \tilde{\mathbf{X}} = (\mathbf{X}^\top \mathbf{X} + \gamma \mathbf{I})^{-1} \mathbf{X}^\top \mathbf{Y}_{(1)} \mathbf{Y}_{(1)}^\top \mathbf{X}$$

and one can check that $\tilde{\mathbf{Y}}_{(i)} \tilde{\mathbf{Y}}_{(i)}^\top = \mathbf{Y}_{(i)} \mathbf{Y}_{(i)}^\top$ for any $i \geq 1$.

The overall Higher-Order Low-Rank Regression procedure (HOLRR) is summarized in Algorithm 1. Note that the Tucker decomposition of the solution returned by HOLRR could be a good initialization point for an Alternative Least Square method. However, studying the theoretical and experimental properties of this approach is beyond the scope of this paper and is left for future work.

Algorithm 1 HOLRR

Input: $\mathbf{X} \in \mathbb{R}^{N \times d_0}$, $\mathcal{Y} \in \mathbb{R}^{N \times d_1 \times \dots \times d_p}$, rank (R_0, R_1, \dots, R_p) and regularization parameter γ .

- 1: $\mathbf{U}_0 \leftarrow$ top R_0 eigenvectors of $(\mathbf{X}^\top \mathbf{X} + \gamma \mathbf{I})^{-1} \mathbf{X}^\top \mathbf{Y}_{(1)} \mathbf{Y}_{(1)}^\top \mathbf{X}$
 - 2: **for** $i = 1$ **to** p **do**
 - 3: $\mathbf{U}_i \leftarrow$ top R_i eigenvectors of $\mathbf{Y}_{(i)} \mathbf{Y}_{(i)}^\top$
 - 4: **end for**
 - 5: $\mathbf{M} = (\mathbf{U}_0^\top (\mathbf{X}^\top \mathbf{X} + \gamma \mathbf{I}) \mathbf{U}_0)^{-1} \mathbf{U}_0^\top \mathbf{X}^\top$
 - 6: $\mathcal{G} \leftarrow \mathcal{Y} \times_1 \mathbf{M} \times_2 \mathbf{U}_1^\top \times_3 \dots \times_{p+1} \mathbf{U}_p^\top$
 - 7: **return** $\mathcal{G} \times_1 \mathbf{U}_0 \times_2 \dots \times_{p+1} \mathbf{U}_p$
-

3.3 Theoretical Analysis

Complexity analysis. We compare the computational complexity of the LRR and HOLRR algorithms. For both algorithms the computational cost for matrix multiplications is asymptotically the same (dominated by the products $\mathbf{X}^\top \mathbf{X}$ and $\mathbf{Y}_{(1)} \mathbf{Y}_{(1)}^\top$). We thus focus our analysis on the computational cost of matrix inversions and truncated singular value decompositions. For the two methods the inversion of the matrix $\mathbf{X}^\top \mathbf{X} + \gamma \mathbf{I}$ can be done in $\mathcal{O}((d_0)^3)$. The LRR method needs to compute the R dominant eigenvectors of a matrix of the same size as $\mathbf{Y}_{(1)} \mathbf{Y}_{(1)}^\top$ (see Section 2.2) which can be done in $\mathcal{O}(R(d_1 d_2 \dots d_p)^2)$. The HOLRR algorithm needs to compute the R_i dominant eigenvectors of the matrix $\mathbf{Y}_{(i)} \mathbf{Y}_{(i)}^\top$ for $i \in [p]$ and to invert the extra matrix $\mathbf{U}_0^\top (\mathbf{X}^\top \mathbf{X} + \gamma \mathbf{I}) \mathbf{U}_0$ of size $R_0 \times R_0$ leading to a complexity of $\mathcal{O}((R_0)^3 + \max_i \{R_i d_i^2\})$. We can conclude that HOLRR is far more efficient than LRR when the output dimensions d_1, \dots, d_p are large.

Approximation guarantees. The following theorem shows that the HOLRR algorithm proposed in the previous section is a $(p+1)$ -approximation algorithm for problem (5).

Theorem 2. *Let \mathcal{W}^* be a solution of problem (5) and let \mathcal{W} be the regression tensor returned by Algorithm 1. If $\mathcal{L} : \mathbb{R}^{d_0 \times \dots \times d_p} \rightarrow \mathbb{R}$ denotes the objective function of (5) w.r.t. \mathcal{W} then $\mathcal{L}(\mathcal{W}) \leq (p+1)\mathcal{L}(\mathcal{W}^*)$.*

Proof. Let $\mathbf{U}_0, \dots, \mathbf{U}_p$ be the matrices defined in Algorithm 1 and let $\mathbf{\Pi}_0, \dots, \mathbf{\Pi}_p$ be the projection matrices defined in problem (7). We have

$$\begin{aligned}
\mathcal{L}(\mathcal{W}) &= \|\mathcal{W} \times_1 \tilde{\mathbf{X}} - \tilde{\mathcal{Y}}\|_F^2 \\
&= \|\tilde{\mathcal{Y}} \times_1 \mathbf{\Pi}_0 \times_2 \cdots \times_{p+1} \mathbf{\Pi}_p - \tilde{\mathcal{Y}}\|_F^2 \\
&\leq \|\tilde{\mathcal{Y}} \times_1 \mathbf{\Pi}_0 \times_2 \cdots \times_{p+1} \mathbf{\Pi}_p - \tilde{\mathcal{Y}} \times_1 \mathbf{\Pi}_0 \times_2 \cdots \times_p \mathbf{\Pi}_{p-1}\|_F^2 \\
&\quad + \|\tilde{\mathcal{Y}} \times_1 \mathbf{\Pi}_0 \times_2 \cdots \times_p \mathbf{\Pi}_{p-1} - \tilde{\mathcal{Y}} \times_1 \mathbf{\Pi}_0 \times_2 \cdots \times_{p-1} \mathbf{\Pi}_{p-2}\|_F^2 \\
&\quad + \cdots + \|\tilde{\mathcal{Y}} \times_1 \mathbf{\Pi}_0 - \tilde{\mathcal{Y}}\|_F^2 \\
&\leq \|\tilde{\mathcal{Y}} \times_{p+1} \mathbf{\Pi}_p - \tilde{\mathcal{Y}}\|_F^2 + \|\tilde{\mathcal{Y}} \times_p \mathbf{\Pi}_{p-1} - \tilde{\mathcal{Y}}\|_F^2 + \cdots + \|\tilde{\mathcal{Y}} \times_1 \mathbf{\Pi}_0 - \tilde{\mathcal{Y}}\|_F^2 ,
\end{aligned}$$

where we used the fact that $\|\mathbf{\Pi M}\|_F \leq \|\mathbf{M}\|_F$ for any projection matrix $\mathbf{\Pi}$. Furthermore, it follows from Theorem 1 that $\mathcal{W}^* = \mathcal{Y} \times_1 \mathbf{\Pi}_0^* \times_2 \cdots \times_{p+1} \mathbf{\Pi}_p^*$ for some projection matrices $\mathbf{\Pi}_i^*$ satisfying the constraints from problem (7). By Proposition 1 each summand in the last inequality is minimal w.r.t. $\mathbf{\Pi}_i$, hence

$$\begin{aligned}
\|\tilde{\mathcal{Y}} \times_i \mathbf{\Pi}_i - \tilde{\mathcal{Y}}\|_F^2 &\leq \|\tilde{\mathcal{Y}} \times_i \mathbf{\Pi}_i^* - \tilde{\mathcal{Y}}\|_F^2 \\
&\leq \|\tilde{\mathcal{Y}} \times_1 \mathbf{\Pi}_0^* \times_2 \cdots \times_{p+1} \mathbf{\Pi}_p^* - \tilde{\mathcal{Y}}\|_F^2 \\
&= \|\mathcal{W}^* \times_1 \tilde{\mathbf{X}} - \tilde{\mathcal{Y}}\|_F^2 \\
&= \mathcal{L}(\mathcal{W}^*)
\end{aligned}$$

which concludes the proof. \square

One direct consequence of this theorem is that if there exists a \mathcal{W}^* such that $\mathcal{W}^* \times_1 \mathbf{X} = \mathcal{Y}$ then Algorithm 1 (using $\gamma = 0$) will return a tensor \mathcal{W} satisfying $\mathcal{W} \times_1 \mathbf{X} = \mathcal{Y}$.

4 HOLRR Kernel Extension

In this section we provide a kernelized version of the HOLRR algorithm. We proceed by analyzing how the algorithm would be instantiated in a feature space and we show that all the steps involved can be performed using the Gram matrix of the input data without having to explicitly compute the feature map.

Let $\phi : \mathbb{R}^{d_0} \rightarrow \mathbb{R}^L$ be a feature map and let $\Phi \in \mathbb{R}^{n \times L}$ be the matrix with lines $\phi(\mathbf{x}^{(n)})^\top$ for $n \in [N]$. The higher-order low-rank regression problem in the feature space boils down to the minimization problem

$$\begin{aligned}
\min_{\mathcal{W} \in \mathbb{R}^{L \times d_1 \times \cdots \times d_p}} \|\mathcal{W} \times_1 \Phi - \mathcal{Y}\|_F^2 + \gamma \|\mathcal{W}\|_F^2 & \quad (8) \\
\text{s.t. } \text{rank}(\mathcal{W}) \leq (R_0, R_1, \dots, R_p) . &
\end{aligned}$$

Following the HOLRR algorithm proposed in Section 3.2 one needs to compute the top R_0 eigenvectors of the $L \times L$ matrix $(\Phi^\top \Phi + \gamma \mathbf{I})^{-1} \Phi^\top \mathbf{Y}_{(1)} \mathbf{Y}_{(1)}^\top \Phi$. The following proposition shows that this can be done using the Gram matrix $\mathbf{K} = \Phi \Phi^\top$ without having to explicitly compute the feature map ϕ .

Proposition 2. If $\alpha \in \mathbb{R}^N$ is an eigenvector with eigenvalue λ of the matrix

$$(\mathbf{K} + \gamma\mathbf{I})^{-1}\mathbf{Y}_{(1)}\mathbf{Y}_{(1)}^\top\mathbf{K} , \quad (9)$$

then $\mathbf{v} = \Phi^\top\alpha \in \mathbb{R}^L$ is an eigenvector with eigenvalue λ of the matrix $(\Phi^\top\Phi + \gamma\mathbf{I})^{-1}\Phi^\top\mathbf{Y}_{(1)}\mathbf{Y}_{(1)}^\top\Phi$.

Proof. Let $\alpha \in \mathbb{R}^N$ be the eigenvector from the hypothesis. We have

$$\begin{aligned} \lambda\mathbf{v} &= \Phi^\top(\lambda\alpha) = \Phi^\top\left((\mathbf{K} + \gamma\mathbf{I})^{-1}\mathbf{Y}_{(1)}\mathbf{Y}_{(1)}^\top\mathbf{K}\right)\alpha \\ &= \Phi^\top(\Phi\Phi^\top + \gamma\mathbf{I})^{-1}\mathbf{Y}_{(1)}\mathbf{Y}_{(1)}^\top\Phi\Phi^\top\alpha \\ &= \left((\Phi^\top\Phi + \gamma\mathbf{I})^{-1}\Phi^\top\mathbf{Y}_{(1)}\mathbf{Y}_{(1)}^\top\Phi\right)\mathbf{v} . \quad \square \end{aligned}$$

Let \mathbf{A} be the top R_0 eigenvectors of the matrix (9). When working with the feature map ϕ , it follows from the previous proposition that line 1 in Algorithm 1 is equivalent to choosing $\mathbf{U}_0 = \Phi^\top\mathbf{A} \in \mathbb{R}^{L \times R_0}$, while the updates in line 3 stay the same. The regression tensor $\mathcal{W} \in \mathbb{R}^{L \times d_1 \times \dots \times d_p}$ returned by this algorithm is then equal to

$$\mathcal{W} = \mathcal{Y} \times_1 \mathbf{P} \times_2 \mathbf{U}_1 \mathbf{U}_1^\top \times_2 \dots \times_{p+1} \mathbf{U}_p \mathbf{U}_p^\top ,$$

where

$$\begin{aligned} \mathbf{P} &= \Phi^\top\mathbf{A} \left(\mathbf{A}^\top\Phi(\Phi^\top\Phi + \gamma\mathbf{I})\Phi^\top\mathbf{A} \right)^{-1} \mathbf{A}^\top\Phi\Phi^\top \\ &= \Phi^\top\mathbf{A} \left(\mathbf{A}^\top\Phi\Phi^\top(\Phi\Phi^\top + \gamma\mathbf{I})\mathbf{A} \right)^{-1} \mathbf{A}^\top\Phi\Phi^\top \\ &= \Phi^\top\mathbf{A} \left(\mathbf{A}^\top\mathbf{K}(\mathbf{K} + \gamma\mathbf{I})\mathbf{A} \right)^{-1} \mathbf{A}^\top\mathbf{K} . \end{aligned}$$

Suppose now that the feature map ϕ is induced by a kernel $k : \mathbb{R}^{d_0} \times \mathbb{R}^{d_0} \rightarrow \mathbb{R}$. The prediction for an input vector \mathbf{x} is then given by $\mathcal{W} \bullet_1 \mathbf{x} = \mathcal{C} \bullet_1 \mathbf{k}_\mathbf{x}$ where the n th component of $\mathbf{k}_\mathbf{x} \in \mathbb{R}^N$ is $k(\mathbf{x}_n, \mathbf{x})$ and the tensor $\mathcal{C} \in \mathbb{R}^{N \times d_1 \times \dots \times d_p}$ is defined by

$$\mathcal{C} = \mathcal{G} \times_1 \mathbf{A} \times_2 \mathbf{U}_1 \times_2 \dots \times_{p+1} \mathbf{U}_p^\top ,$$

with $\mathcal{G} = \mathcal{Y} \times_1 \left(\mathbf{A}^\top\mathbf{K}(\mathbf{K} + \gamma\mathbf{I})\mathbf{A} \right)^{-1} \mathbf{A}^\top\mathbf{K} \times_2 \mathbf{U}_2^\top \times_3 \dots \times_{p+1} \mathbf{U}_p$.

Now, let \mathcal{H} be the reproducing kernel Hilbert space associated with the kernel k . The overall procedure for kernelized HOLRR is summarized in Algorithm 2. This algorithm returns the tensor $\mathcal{C} \in \mathbb{R}^{N \times d_1 \times \dots \times d_p}$ defining the regression function

$$f : \mathbf{x} \mapsto \mathcal{C} \bullet_1 \mathbf{k}_\mathbf{x} = \sum_{n=1}^N k(\mathbf{x}, \mathbf{x}^{(n)}) \mathcal{C}^{(n)} ,$$

where $\mathcal{C}^{(n)} = \mathcal{C}_{n, \dots} \in \mathbb{R}^{d_1 \times \dots \times d_p}$.

Algorithm 2 Kernelized HOLRR

Input: Gram matrix $\mathbf{K} \in \mathbb{R}^{N \times N}$, $\mathcal{Y} \in \mathbb{R}^{N \times d_1 \times \dots \times d_p}$, rank (R_0, R_1, \dots, R_p) and regularization parameter γ .

- 1: $\mathbf{A} \leftarrow$ top R_0 eigenvectors of $(\mathbf{K} + \gamma \mathbf{I})^{-1} \mathbf{Y}_{(1)} \mathbf{Y}_{(1)}^\top \mathbf{K}$
- 2: **for** $i = 1$ **to** p **do**
- 3: $\mathbf{U}_i \leftarrow$ top R_i eigenvectors of $\mathbf{Y}_{(i)} \mathbf{Y}_{(i)}^\top$
- 4: **end for**
- 5: $\mathbf{M} \leftarrow (\mathbf{A}^\top \mathbf{K} (\mathbf{K} + \gamma \mathbf{I}) \mathbf{A})^{-1} \mathbf{A}^\top \mathbf{K}$
- 6: $\mathcal{G} \leftarrow \mathcal{Y} \times_1 \mathbf{M} \times_2 \mathbf{U}_1^\top \times_3 \dots \times_{p+1} \mathbf{U}_p^\top$
- 7: **return** $\mathcal{C} = \mathcal{G} \times_1 \mathbf{A} \times_2 \mathbf{U}_1 \times_3 \dots \times_{p+1} \mathbf{U}_p$

Table 1: Average running time for different size of the regression tensor \mathcal{W} . Each line comes from one of the experiments. The times reported are the average learning times in seconds for a training set of size 100.

| SIZE OF \mathcal{W} | RLS | LRR | ADMM | MLMT-NC | HOLRR |
|------------------------------------|-------|-------|-------|---------|-------|
| $10 \times 10 \times 10 \times 10$ | 0.012 | 0.45 | 12.92 | 945.79 | 0.04 |
| $3 \times 70 \times 70$ | 0.04 | 10.46 | — | — | 0.08 |
| $160 \times 5 \times 16 \times 5$ | 2.07 | 2.24 | 40.23 | — | 1.67 |

5 Experiments

We present and analyze the experimental results obtained on a regression task on synthetic data, an image reconstruction task and a meteorological forecasting task on real data¹. We compare the predictive accuracy of HOLRR with the following methods:

- RLS: Regularized least squares.
- LRR: Low-rank regression (see Section 2.2).
- ADMM: a multilinear approach based on tensor trace norm regularization introduced in (Gandy et al., 2011) and (Romera-Paredes et al., 2013).
- MLMT-NC: a nonconvex approach proposed in (Romera-Paredes et al., 2013) in the context of multilinear multitask learning.

For experiments with kernel algorithms we use the readily available kernelized RLS and the LRR kernel extension proposed in (Mukherjee & Zhu, 2011) (note that ADMM and MLMT-NC only consider a linear dependency between inputs and outputs).

Although MLMLT-NC is perhaps the closest algorithm to ours, we applied it only to simulated data. This is because MLMLT-NC is computationally very expensive and becomes intractable for large data sets. To give an idea on the running times, averages for some of the experiments are reported in Table 1.

¹The code and data used in the experiments will be made available by the authors.

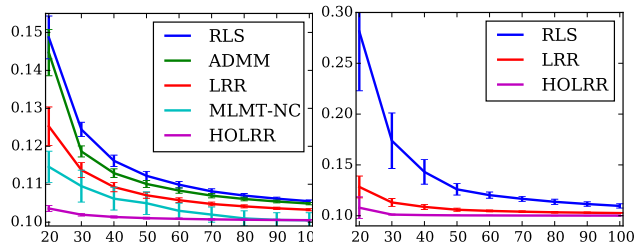


Figure 1: Average RMSE as a function of the training set size: (left) linear data, (right) nonlinear data.

5.1 Synthetic Data

We generate both linear and nonlinear data. The linear data is drawn from the model $\mathcal{Y} = \mathcal{W} \bullet_1 \mathbf{x} + \mathcal{E}$ where $\mathcal{W} \in \mathbb{R}^{10 \times 10 \times 10 \times 10}$ is a tensor of multilinear rank $(6, 4, 4, 8)$ drawn at random, $\mathbf{x} \in \mathbb{R}^{10}$ is drawn from $\mathcal{N}(0, \mathbf{I})$ and each component of the error tensor \mathcal{E} is drawn from $\mathcal{N}(0, 0.1)$. The nonlinear data is drawn from the model $\mathcal{Y} = \mathcal{W} \bullet_1 (\mathbf{x} \otimes \mathbf{x}) + \mathcal{E}$ where $\mathcal{W} \in \mathbb{R}^{25 \times 10 \times 10 \times 10}$ is a tensor of rank $(5, 6, 4, 2)$ drawn at random and $\mathbf{x} \in \mathbb{R}^5$ and \mathcal{E} are generated as above. The hyper-parameters for all algorithms are selected using 3-fold cross validation on the training data.

These experiments have been carried out for different sizes of the training data set, 20 trials have been executed for each size. The average RMSEs on a test set of size 100 for the 20 trials are reported in Figure 1. We see that the HOLRR algorithm clearly outperforms the other methods on the linear data. MLMT-NC is the method obtaining the better accuracy after ours, it is however much more computationally expensive (see Table 1). On the nonlinear data the LRR method achieves good performances but HOLRR is still significantly more accurate for small data set sizes.

5.2 Image Reconstruction from Noisy Measurements

To give an illustrative intuition on the differences between matrix and multilinear rank regularization we generate data from the model $\mathcal{Y} = \mathcal{W} \bullet_1 \mathbf{x} + \mathcal{E}$ where the tensor \mathcal{W} is a color image of size $m \times n$ encoded with three color channels RGB. We consider two different tasks depending on the input dimension: (i) $\mathcal{W} \in \mathbb{R}^{3 \times m \times n}$, $\mathbf{x} \in \mathbb{R}^3$ and (ii) $\mathcal{W} \in \mathbb{R}^{n \times m \times 3}$, $\mathbf{x} \in \mathbb{R}^n$. In both tasks the components of both \mathbf{x} and \mathcal{E} are drawn from $\mathcal{N}(0, 1)$ and the regression tensor \mathcal{W} is learned from a training set of size 200.

This experiment allows us to visualize the tensors returned by the RLS, LRR and HOLRR algorithms. The results are shown in Figure 2 for three images: a green cross (of size 50×50), a thumbnail of a Rothko painting (44×70) and a square made of triangles (70×70), note that the first two images have a low rank structure which is not the case for the third one.

We first see that HOLRR clearly outperforms LRR on the task where the

input dimension is small (task (i)). This is to be expected since the rank of the matrix $\mathbf{W}_{(1)}$ is at most 3 and LRR is unable to enforce a low-rank structure on the output modes of \mathcal{W} . When the rank constraint is set to 1 for LRR and (3, 1, 1) for HOLRR we clearly see that unlike HOLRR the LRR approach does not enforce any low-rank structure on the regression tensor along the output modes. On task (ii) the difference is more subtle, but we can see that setting a rank constraint of 2 for the LRR algorithm prevents the model from capturing the white border around the green cross and creates the vertical lines artifact in the Rothko painting. For higher values of the rank the model starts to learn the noise. The tensor returned by HOLRR with rank (4, 4, 3) does not exhibit these behaviors and gives better results on these two images. On the square image which does not have a low-rank structure both algorithms do not perform very well. Overall, we see that capturing the multilinear low-rank structure of the output data allows HOLRR to separate the noise from the true signal better than RLS and LRR.

5.3 Real Data

We compare our algorithm with other methods on the task of meteo forecasting. We collected data from the meteorological office of the UK ²: monthly average measurements of 5 variables in 16 stations across the UK from 1960 to 2000. The forecasting task consists in predicting the values of the 5 variables in the 16 stations from their values in the preceding months. We use the values of all the variables from the past 2 months as covariates and consider the tasks of predicting the values of all variables for the next k months, the output tensors are thus in $\mathbb{R}^{k \times 16 \times 5}$.

We randomly split the available data into a training set of size N , a test set of size 50 and a validation set of size 20, for all methods hyper-parameters are chosen w.r.t. to their performance on the validation set. The average test RMSE over 10 runs of this experiment for different values of N and k are reported in Table 2. We see that the HOLRR has overall a better predictive accuracy than the other methods, especially when the tensor structure of the output data gets richer ($k = 3$ and $k = 5$). On this dataset, nonlinear methods only improve the results by a small margin with the RBF kernel, and the polynomial kernel performs poorly.

6 Conclusion

We proposed a low-rank multilinear regression model for tensor-structured output data. We developed a fast and efficient algorithm to tackle the multilinear rank penalized minimization problem and provided theoretical approximation guarantees. Experimental results showed that capturing low-rank structure in the output data can help to improve tensor regression performance.

²<http://www.metoffice.gov.uk/public/weather/climate-historic/>

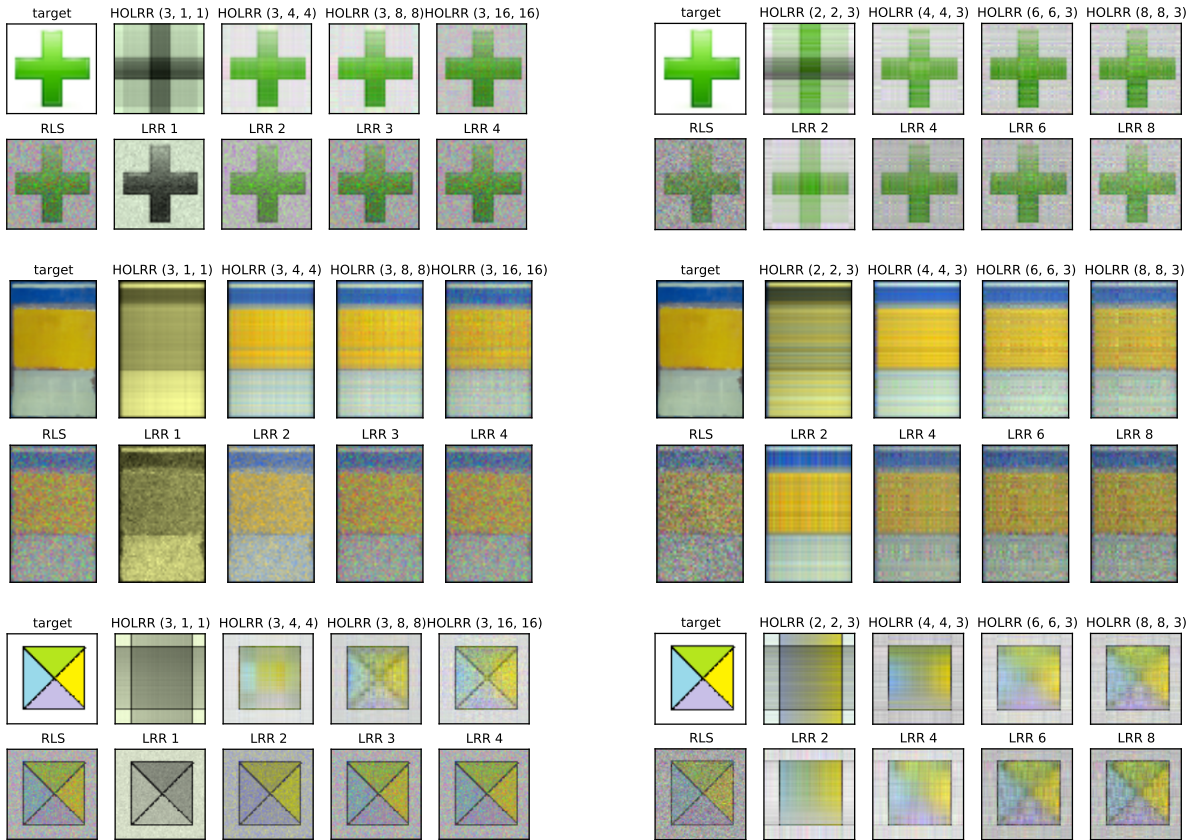


Figure 2: Image reconstruction from noisy measurements: $\mathcal{Y} = \mathcal{W} \bullet_1 \mathbf{x} + \mathcal{E}$ where \mathcal{W} is a color image (RGB). (left) Task (i): input dimension is the number of channels. (right) Task (ii): input dimension is the height of the image. Each image is labeled with the name of the algorithm followed by the value used for the rank constraint.

References

- Anderson, T. W. Estimating linear restrictions on regression coefficients for multivariate normal distributions. *Annals of Mathematical Statistics*, 22:327–351, 1951.
- Bahadori, M. T., Yu, Q. R., and Liu, Y. Fast multivariate spatio-temporal analysis via low rank tensor learning. In *NIPS*. 2014.
- Cichocki, A., Zdunek, R., Phan, A.H., and Amari, S.I. *Nonnegative Matrix and Tensor Factorizations*. Applications to Exploratory Multi-way Data Analysis and Blind Source Separation. Wiley, 2009.
- De Lathauwer, Lieven, De Moor, Bart, and Vandewalle, Joos. A multilinear

Table 2: Forecasting experiment: the task is to predict the values for all variables for the next k months using a training set of size N .

| $k = 1, N = 50$ | ADMM | RLS | LRR | HOLRR |
|------------------|---------------|--------|---------------|---------------|
| LINEAR | 0.6323 | 0.6481 | <u>0.6261</u> | 0.6310 |
| RBF | - | 0.6081 | 0.6076 | 0.6035 |
| POLY | - | 0.6580 | <u>0.6526</u> | 0.6793 |
| $k = 1, N = 100$ | ADMM | RLS | LRR | HOLRR |
| LINEAR | <u>0.5997</u> | 0.6218 | <u>0.6003</u> | <u>0.6003</u> |
| RBF | - | 0.5926 | 0.5920 | 0.5808 |
| POLY | - | 0.6230 | <u>0.6160</u> | 0.6222 |
| $k = 3, n = 50$ | ADMM | RLS | LRR | HOLRR |
| LINEAR | 0.6367 | 0.6683 | 0.6256 | <u>0.6163</u> |
| RBF | - | 0.6297 | 0.6296 | 0.6096 |
| POLY | - | 0.6587 | 0.6412 | <u>0.6355</u> |
| $k = 3, N = 100$ | ADMM | RLS | LRR | HOLRR |
| LINEAR | 0.6269 | 0.6740 | 0.6186 | 0.6086 |
| RBF | - | 0.6153 | 0.6090 | 0.6015 |
| POLY | - | 0.6588 | 0.6439 | <u>0.6379</u> |
| $k = 5, N = 50$ | ADMM | RLS | LRR | HOLRR |
| LINEAR | 0.6302 | 0.6719 | 0.6232 | <u>0.6127</u> |
| RBF | - | 0.6150 | 0.6192 | 0.6017 |
| POLY | - | 0.6579 | <u>0.6338</u> | 0.6353 |
| $k = 5, N = 100$ | ADMM | RLS | LRR | HOLRR |
| LINEAR | 0.6140 | 0.6449 | 0.6021 | <u>0.5971</u> |
| RBF | - | 0.6020 | 0.5908 | 0.5886 |
| POLY | - | 0.6432 | 0.6202 | <u>0.6107</u> |

singular value decomposition. *SIAM journal on Matrix Analysis and Applications*, 21(4):1253–1278, 2000.

Gandy, Silvia, Recht, Benjamin, and Yamada, Isao. Tensor completion and low-n-rank tensor recovery via convex optimization. *Inverse Problems*, 27(2):025010, 2011.

Izenman, A. J. Reduced-rank regression for the multivariate linear model. *Journal of Multivariate Analysis*, 5(2):248–264, 1975.

Izenman, A. J. *Modern Multivariate Statistical Techniques: Regression, Classification, and Manifold Learning*. Springer-Verlag, New York, 2008.

Kolda, T. G. and Bader, B. W. Tensor decompositions and applications. *SIAM review*, 51(3):455–500, 2009.

Lu, H., Plataniotis, K.N., and Venetsanopoulos, A. *Multilinear Subspace Learning: Dimensionality Reduction of Multidimensional Data*. CRC Press, 2013.

Mukherjee, A. and Zhu, J. Reduced rank ridge regression and its kernel extensions. *Statistical analysis and data mining*, 4(6):612–622, 2011.

Reinsel, G.C. and Velu, R.P. *Multivariate reduced-rank regression: theory and applications*. Lecture Notes in Statistics. Springer, 1998.

- Romera-Paredes, B., Aung, M. H., Bianchi-Berthouze, N., and Pontil, M. Multilinear multitask learning. In *Proceedings of the 30th International Conference on Machine Learning (ICML-13)*, pp. 1444–1452, 2013.
- Signoretto, M., Dinh, Q. T., De Lathauwer, L., and Suykens, J. K. Learning with tensors: a framework based on convex optimization and spectral regularization. *Machine Learning*, pp. 1–49, 2013.
- Zhou, H., Li, L., and Zhu, H. Tensor regression with applications in neuroimaging data analysis. *Journal of the American Statistical Association*, 108(502): 540–552, 2013.